Journal of The Electrochemical Society

Lithium-Ion Cells Assembled with Flexible Hybrid Membrane Containing Li^+-Conducting Lithium Aluminum Germanium Phosphate

Lithium-Ion Cells Assembled with Flexible Hybrid Membrane Containing Li^+-Conducting Lithium Aluminum Germanium Phosphate

Seul-Ki Kim,[a] Yun-Chae Jung,[a] Duck-Hyun Kim,[b] Woo-Cheol Shin,[b] Makoto Ue,[b,*] and Dong-Won Kim[a,*,z]

[a]*Department of Chemical Engineering, Hanyang University, Seungdong-gu, Seoul 133-791, Korea*
[b]*Energy 2 Lab, Battery R&D Center, Samsung SDI, Gyeonggi-do 443-803, Korea*

Hybrid membranes composed of 90 wt% Li^+-conducting inorganic electrolyte (lithium aluminum germanium phosphate, LAGP) and 10 wt% poly(vinylidene fluoride-co-hexafluoropropylene) (P(VdF-co-HFP)) polymer were prepared in the form of a flexible thin film and directly formed on the as-prepared negative electrode. The lithium-ion cells assembled with the hybrid membrane exhibited superior cycling performance in terms of discharge capacity, capacity retention, rate capability and high temperature cycling stability, as compared to the cell with polypropylene separator and liquid electrolyte. The use of hybrid membranes allowed improve thermal properties compared to conventional polyolefin separator and use less amount of flammable liquid electrolyte, resulting in enhancement of thermal safety of the cell.

 [DOI: 10.1149/2.0831606jes]

Manuscript submitted January 20, 2016; revised manuscript received March 3, 2016. Published March 15, 2016.

Lithium-ion batteries have been predominantly used as power sources for portable electronic devices and are now being extensively developed as potential power sources for electric vehicles and energy storage systems because of their high energy density and long cycle life.[1–8] However, the full utilization of these batteries is still challenging for future large-capacity energy storage applications due to the safety issues caused by the flammable nature of the liquid electrolyte.[9] In addition, the polyolefin separators used in current lithium-ion batteries may shrink and even melt at elevated temperatures, which causes a short circuit between two electrodes in cases where unusually high heat is generated, leading to fire and explosion.[10–12] Furthermore, the large difference in polarity between hydrophobic polyolefin separators without surface treatment and polar organic solvents leads to poor wettability, resulting in high ionic resistance during cycling.[13] In this respect, extensive studies have been carried out on inorganic solid electrolytes without a polymer separator as an alternative electrolyte for improving the safety of lithium-ion batteries.[14–18] However, many inorganic materials require a thermal sintering at high temperatures to form a pellet-type solid electrolyte. In addition, a lack of flexibility results in poor interfacial contact between the inorganic solid electrolyte and solid electrodes in the cell during charge and discharge cycling. To solve these problems, the hybrid solid electrolytes composed of an inorganic electrolyte and flexible polymer have been investigated.[19–23] However, it is still challenging to secure competitive cycling performance when compared to liquid electrolyte-based lithium-ion batteries. The most critical issue to be solved in cells employing an inorganic electrolyte is high interfacial resistances between electrolyte and electrodes due to the solid-on-solid interface in the cells. Therefore, it is highly desirable to minimize the interfacial resistances at solid-solid interfaces while enhancing battery safety and maintaining a cycling performance competitive to that of lithium-ion batteries that employ conventional polyolefin separator and organic liquid electrolyte. As et al. reported that the use of a hybrid electrolyte composed of 90 wt% inorganic solid electrolyte and 10 wt% organic liquid electrolyte could effectively reduce the solid-on-solid interfaces.[24] In our previous study, the hybrid separators based on a garnet-structured lithium ion conductor (lithium lanthanum zirconium oxide, LLZO) were applied to a lithium-ion cell composed of a graphite negative electrode and a $LiCoO_2$ positive electrode.[25] The cell assembled with a hybrid separator containing liquid electrolyte exhibited good cycling performance and enhanced safety compared to those of a cell with a polyolefin separator and liquid electrolyte. The hybrid separator was prepared by directly casting a slurry containing LLZO, poly(vinylidene fluoride-co-hexafluoropropylene) (P(VdF-co-HFP)) and dibutyl phthalate (DBP) in acetone onto the as-prepared negative electrode. In this process, DBP used as a pore-forming agent must be extracted by immersing the hybrid separator applied on the negative electrode in methanol. However, this approach may destroy the structure of the as-prepared negative electrode during immersion in methanol and give rise to the complexity of fabricating the batteries as well as increase the manufacturing cost.

In this work, we prepared hybrid membranes composed of lithium aluminum germanium phosphate (LAGP) and P(VdF-co-HFP) copolymer by a dry phase inversion process without extraction of DBP.[26–29] Herein, LAGP was used as a Li^+-conducting inorganic electrolyte, since it had higher ionic conductivity than LLZO.[30] The casting slurry composed of LAGP, P(VdF-co-HFP), acetone (solvent) and octane (non-solvent) was directly applied onto the as-prepared negative graphite electrode to enhance interfacial adhesion and lower interfacial resistance, and pores were formed in the hybrid membrane through dry phase inversion. In this process, the porosity of the hybrid membrane could be controlled by simply adjusting the ratio of octane to acetone. Lithium-ion cells employing a graphite negative electrode, a hybrid membrane containing a small amount of liquid electrolyte and a $LiNi_{0.5}Co_{0.2}Mn_{0.3}O_2$ positive electrode were assembled, and their cycling performance was evaluated and compared to those of a cell assembled with a conventional polypropylene (PP) separator and liquid electrolyte. Our results demonstrate that the lithium-ion cells assembled with a hybrid membrane containing Li^+-conducting LAGP exhibits good cycling performance in terms of discharge capacity, capacity retention, rate capability and cycling stability at high temperatures. The hybrid membrane also endowed the cell with good protection against an internal short circuit at elevated temperature.

Experimental

Preparation of hybrid membrane.—Li^+-conducting LAGP ($Li_{1.5}Al_{0.5}Ge_{1.5}(PO_4)_3$) powder was synthesized by a conventional solid solution method.[31] A stoichiometric mixture of lithium carbonate, aluminum oxide, germanium oxide and ammonium dihydrogen phosphate was used as the starting materials for the synthesis of LAPG. A small amount of B_2O_3 (0.05 wt% B_2O_3 to LAGP) was added in order to increase the ionic conductivity of LAGP. The powder mixture

*Electrochemical Society Member.
[z]E-mail: dongwonkim@hanyang.ac.kr

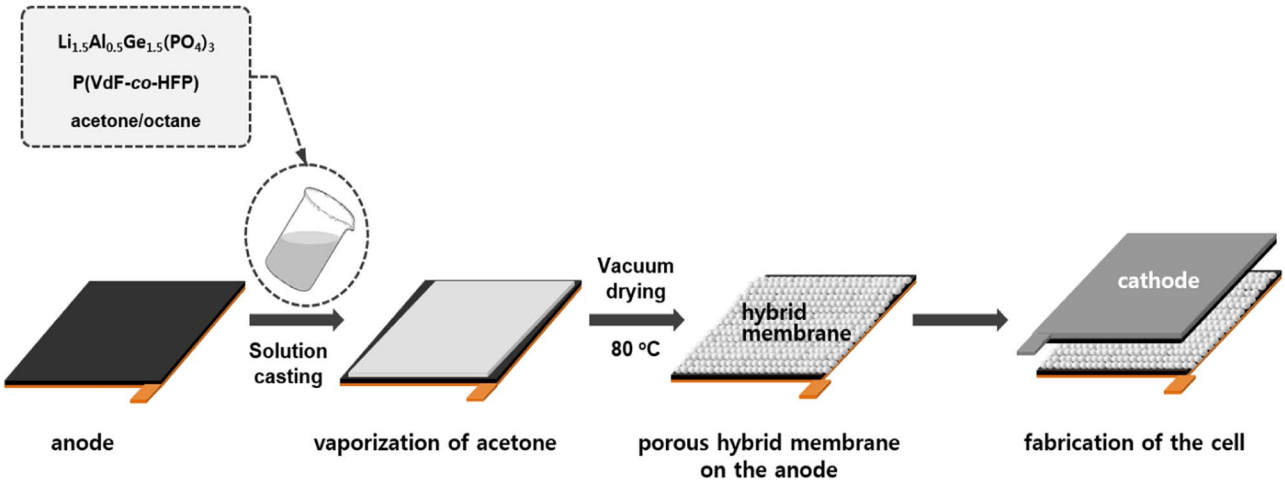

Figure 1. Schematic presentation for fabrication of a lithium-ion cell using a hybrid membrane. The hybrid membrane was directly formed on the as-prepared negative electrode by solution casting and the dry phase inversion method.

was first thoroughly dispersed in isopropyl alcohol by ballmilling for 24 h and dried at 25°C for 24 h to evaporate the volatile solvent. The powder mixture was heated to 700°C at a heating rate of 5°C min^{-1} in a tube furnace and held at that temperature for 2 h to release any volatile compounds. The powders were then ground, followed by heating to 850°C with a heating rate of 5°C min^{-1} and calcinated at the same temperature for 12 h in an argon atmosphere. LAGP was finally obtained as a fine white powder. A hybrid membrane was prepared by solution casting and dry phase inversion method, as schematically illustrated in Figure 1. LAGP and P(VdF-co-HFP) (Mw = 470,000, Kynar Flex 2801, Arkema) (90/10 by weight) were added into an acetone solvent containing octane as a non-solvent, and the solution was mixed using ballmilling for 12 h. In preparing the coating slurry, the amount of octane was adjusted to control the porosity of the hybrid membrane, as given in Table I. When the complete homogenization of the mixture had occurred, the slurry was cast using a doctor blade on the as-prepared graphite negative electrode by allowing evaporation of the acetone solvent at room temperature. After 1 h, it was further vacuum dried at 80°C for 12 h in order to remove octane and form pores in the hybrid membrane. The thickness of the hybrid membranes was controlled to 35 μm. A freestanding hybrid membrane was also prepared in order to investigate its characteristics by solution casting on a flat glass plate, following a dry phase inversion process.

Electrode preparation and cell assembly.—The positive electrode was prepared by coating an N-methyl pyrrolidone (NMP)-based slurry containing $LiNi_{0.5}Co_{0.2}Mn_{0.3}O_2$, poly(vinylidene fluoride) (PVdF) and super-P carbon (MMM Co.) (85:7.5:7.5 by weight) onto aluminum foil. The active mass loading in the positive electrode corresponded to a capacity of 2.95 mAh cm^{-2}. The negative electrode was similarly prepared by coating an NMP-based slurry of graphite, PVdF and super-P carbon (88:8:4 by weight) onto a copper foil. The hybrid membranes were directly formed on the graphite negative electrode, as described above. The lithium-ion cell was then assembled with a positive $LiCoO_2$ electrode and a hybrid membrane formed on the negative electrode. The cell was enclosed in a pouch injected with electrolyte solution and was then vacuum-sealed. A liquid electrolyte, which consisted of 1.15 M $LiPF_6$ in ethylene carbonate (EC)/diethyl carbonate (DEC) (3:7 by volume, battery grade), was kindly supplied by PANAX ETEC Co. Ltd., and was used without further treatment. For comparison, the lithium-ion cell was also fabricated with a conventional PP separator (Celgard 2400) and the same liquid electrolyte (1.15 M $LiPF_6$-EC/DEC). All cells were assembled in a dry box filled with argon gas.

Table I. Composition of the casting slurry in preparing hybrid membranes.

Membrane	LAGP (g)	P(VdF-co-HFP) (g)	Acetone (g)	Octane (g)
HM-1[a]	90	10	20	0
HM-2	90	10	20	1
HM-3	90	10	20	2
HM-4	90	10	20	3

[a]HM stands for a hybrid membrane.

Characterization and measurements.—A cross-section polisher (JEOL IB-09010CP) was used to prepare the cross-section of the hybrid membrane. Its cross-sectional morphology was examined using a scanning electron microscope (SEM, JEOL JSM-6300). The elemental distribution on the cross-sectional area of hybrid membrane was examined using energy dispersive X-ray spectroscopy (EDS). X-ray diffraction (XRD) patterns of LAGP, P(VdF-co-HFP) and hybrid membranes were obtained using an X-ray diffractometer (Rigaku M2500) with Cu Kα radiation. The porosity of the hybrid membranes was determined using an n-butanol uptake method.[32,33] In order to measure electrolyte uptake, the hybrid membrane was immersed in the liquid electrolyte for 1 h. Afterwards, it was taken out from the electrolyte solution, and the uptake of the electrolyte solution was then determined by measuring the weights of the membrane before and after soaking in the liquid electrolyte, respectively.[34] The thermal shrinkage of the hybrid membranes was measured in terms of their dimensional changes after being held at 150°C for 1 h.[35] The self-extinguishing time (SET) was measured to compare the flammability of hybrid membrane and PP separator.[36,37] Briefly, SET was obtained by igniting the pre-weighed hybrid membrane and PP separator soaked with liquid electrolyte, followed by recording the time it took for the flame to extinguish. AC impedance measurements were performed to measure the ionic conductivity and interfacial resistance using a Zahner Electrik IM6 impedance analyzer over a frequency range of 100 kHz to 1 mHz with an amplitude of 10 mV. Charge and discharge cycling tests of the lithium-ion cells were conducted at a constant current rate (0.5 C) over a voltage range of 3.0 to 4.3 V using battery testing equipment (WBCS 3000, Wonatech) at 25 and 55°C, respectively. As for the rate capability, the cells were charged at a 0.2 C rate and discharged at 0.1, 0.2, 0.5, 1.0 and 2.0 C rates. The HF content in the electrolyte was measured by an acid-base titration method after the cell was stored in a 55°C oven for a week.[38] Methyl orange was used as an acid-base indicator. To investigate the thermal stability of the hybrid membranes, the cells were charged to 4.3 V and

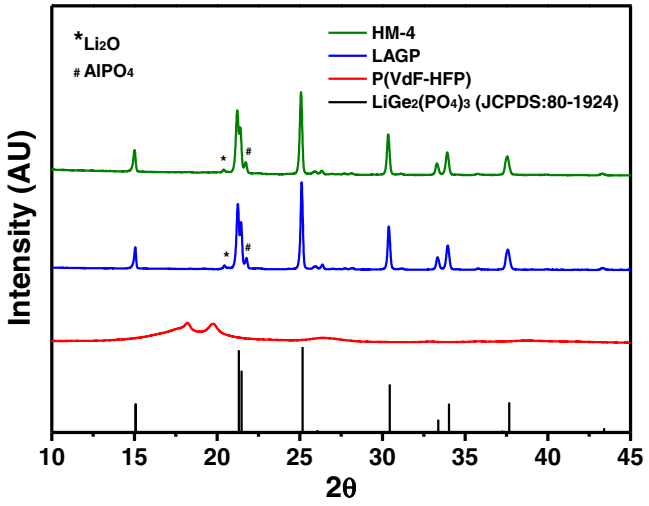

Figure 2. XRD patterns of LAGP, P(VdF-co-HFP) and hybrid membrane (HM-4).

placed in an oven at 150°C. The open circuit voltage of cells was then recorded as a function of storage time.[39]

Results and Discussion

Figure 2 shows the XRD patterns of LAGP, P(VdF-co-HFP) and hybrid membrane (HM-4). The XRD pattern obtained from LAGP closely matched the standard pattern of the NASICON-type $LiGe_2(PO_4)_3$ (JCPDS 80–1924), with minor impurity peaks corresponding to Li_2O and $AlPO_4$.[31] The hexagonal lattice parameters of the LAGP crystalline phase could be obtained from a least-squares fitting. The lattice parameters for the LAGP crystalline phase were calculated to be a = 8.286 ± 0.002 Å and c = 20.535 ± 0.036 Å, respectively. These values are well consistent with those (a = 8.250 Å and c = 20.460 Å) previously reported for $LiGe_2(PO_4)_3$.[40] The replacement of the Ge^{4+} (0.530 Å) by the larger Al^{3+} (0.535 Å) in the $LiGe_2(PO_4)_3$ crystalline phase resulted in structural modification that expands the lattice parameters.[40,41] The XRD pattern of P(VdF-co-HFP) presents three broad peaks at 2θ = 18.2°, 19.8°, 26.5°, which are corresponding to σ, β and γ crystalline phases of PVdF, respectively.[42] The intensity of crystalline peaks in P(VdF-co-HFP) was significantly reduced by hybridizing with LAGP, which can be attributed to the destruction effect of LAGP on the ordered arrangement of the polymer chains. The crystalline peaks of LAGP in hybrid membrane were almost the same without any broadening or shifting, indicating that the LAGP powder maintains its crystalline structure without any degradation in the hybrid membrane.

A cross-sectional FE-SEM image of the representative hybrid membrane (HM-4) is presented in Figure 3a. The hybrid membrane had a submicron pore structure, which enabled the absorption of liquid electrolyte into the porous membrane. It confirmed that the hybrid membrane is mainly composed of LAGP powders. Despite the high content of LAGP powders (90 wt%), the resulting hybrid membrane was obtained as a freestanding and flexible thin film, as demonstrated in the inset of Figure 3a, which means that 10 wt% P(VdF-co-HFP) is enough for binding the inorganic LAGP powders and making a flexible thin film. Figures 3b–3e show the EDS mapping images of various elements (Ge, P, O and F) on the cross-section of the hybrid membrane shown in Figure 3a. It can be seen that Ge, P and O elements arising from the LAGP powders are overwhelmingly distributed across the image. The fluorine elements from P(VdF-co-HFP) polymer are also uniformly dispersed in the hybrid membrane. These results suggest that LAGP powders are homogeneously distributed and well embedded in the porous hybrid membrane.

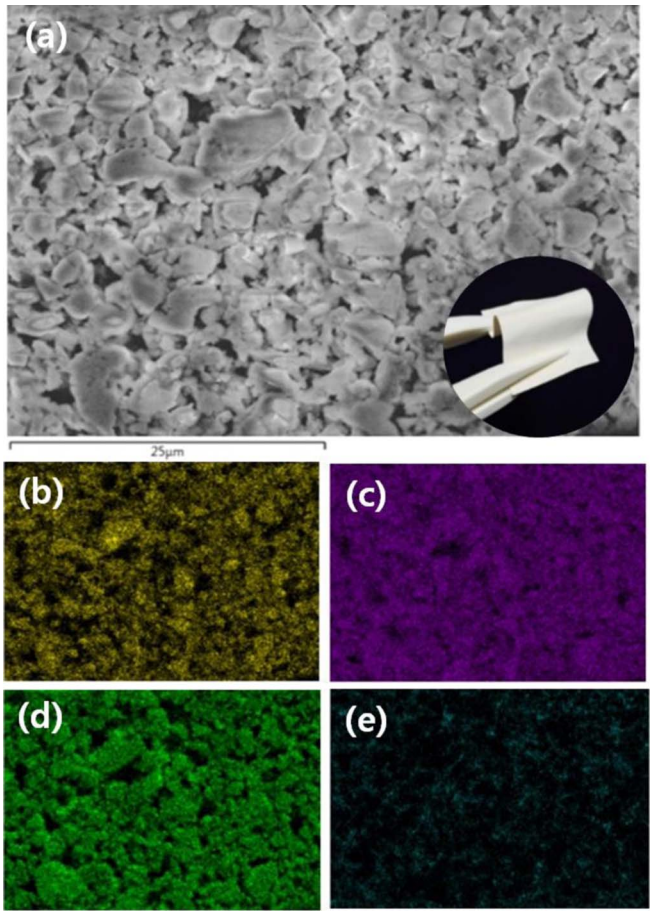

Figure 3. (a) Cross-sectional FE-SEM image of the hybrid membrane (HM-4) and EDS mapping images of (b) Ge, (c) P, (d) O and (e) F elements on its cross-section. The hybrid membrane was obtained as flexible thin film, as demonstrated in the inset of (a).

Figure 4 shows the SEM images of the cross-sectional area for hybrid membrane (HM-4) cast on carbon negative electrode with two different magnifications. The interfacial contact between hybrid membrane and carbon electrode was very firm without separation into membrane and electrode, since the hybrid membrane was directly formed onto the negative electrode via solution casting. Good adhesion to the negative electrode can decrease the interfacial resistances and reduce the lithium dendrite formation on the negative electrode.

The porosity, electrolyte uptake and ionic conductivities of various hybrid membranes soaked with liquid electrolyte are given in Table II. The porosity of the hybrid membranes increased from 19.2 to 38.1% with increasing content of octane. Since the octane is less volatile than acetone, the evaporation of acetone at room temperature resulted in increased concentrations of polymer and octane, which

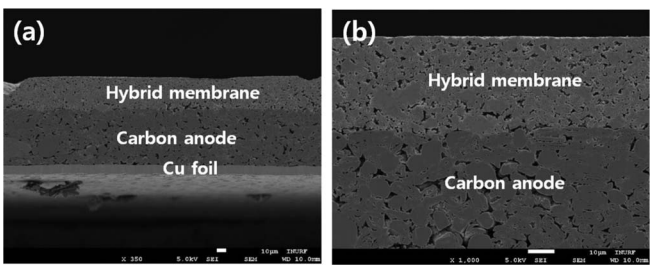

Figure 4. SEM images of the cross-sectional area for hybrid membrane (HM-4) formed on carbon electrode with two different magnifications.

Table II. The porosity, electrolyte uptake and ionic conductivities of the PP separator and hybrid membranes soaked with liquid electrolyte.

Membrane	Thickness (μm)	Porosity (%)	Electrolyte uptake (%)	Ionic conductivity (S cm^{-1})
PP	25	41.0	80.3	4.5×10^{-4}
HM-1	35	19.2	12.5	5.6×10^{-4}
HM-2	35	31.4	18.0	8.3×10^{-4}
HM-3	35	35.9	20.6	9.8×10^{-4}
HM-4	35	38.1	22.4	1.1×10^{-3}

caused a phase separation. When octane was evaporated under a vacuum at 80°C, pores were formed at the locations where the octane rich phase had existed. Thus, the porosity of the hybrid membrane was increased with increasing content of non-solvent (octane). The uptake of electrolyte solution in the hybrid membranes was much lower than that of the PP separator, due to their lower porosity and higher skeletal density. Even though their porosity and electrolyte uptake were lower, the ionic conductivities were higher in the hybrid membranes than that measured in the PP separator. This result suggests that the Li^+-conductive LAGP particles in the hybrid membrane contributes to the ionic conductivity. In addition, the facile ionic conduction in the gel polymer electrolyte phase formed by P(VdF-co-HFP) and liquid electrolyte can also contribute to the high ionic conductivity. Thus, higher ionic conductivity in the hybrid membranes employing LAGP powders and P(VdF-co-HFP) arises from a combination of solid electrolyte (LAGP) and gel polymer electrolyte, and not from the liquid electrolyte alone. It should be noted that the amount of liquid electrolyte in the hybrid membrane is quite low compared to the PP separator soaked with liquid electrolyte. For example, the hybrid electrolyte prepared with HM-4 is composed of 73.5 wt% inorganic electrolyte, 8.2 wt% P(VdF-co-HFP) polymer and 18.3 wt% liquid electrolyte.

A hybrid membrane was used to assemble the lithium-ion cell composed of a graphite negative electrode and a $LiNi_{0.5}Co_{0.2}Mn_{0.3}O_2$ positive electrode. Figure 5a shows the typical charge-discharge curves of the lithium-ion cell assembled with HM-4 at 25°C. The cell delivered an initial discharge capacity of 157.6 mAh g^{-1} based on the active $LiNi_{0.5}Co_{0.2}Mn_{0.3}O_2$ material in the positive electrode. The discharge capacity of the cell declined to 136.9 mAh g^{-1} after 200 cycles, which corresponded to 86.9% of the initial discharge capacity. Figure 5b shows the discharge capacities of lithium-ion cells assembled with PP separator and different hybrid membranes, as a function of cycle number. The capacity retention of the cells with hybrid membranes ranged from 84.3 to 86.9% after 200 cycles. Compared with 76.8% retention of the cell assembled with PP separator and liquid electrolyte, they provided better cycling stability. The good cycling stability can be ascribed to enhanced interfacial contacts between the membrane and the electrode, as demonstrated in Figure 4. Further, the encapsulation of a small amount of liquid electrolyte in the hybrid membrane prevented exudation of the electrolyte solution, as well as suppressed harmful interfacial side reactions between the electrodes and the electrolyte during the repeated cycling, which resulted in better capacity retention.

Rate capability of the lithium-ion cells assembled with the PP separator and HM-4 was evaluated and compared. The cells were charged to 4.3 V at a constant current rate of 0.2 C, followed by a constant voltage charge, and then discharged at different current rates ranging from 0.1 to 2.0 C. Figures 6a and 6b show the discharge curves of the cell with PP separator and HM-4, respectively, as a function of the C rate. It is evident that the cell with HM-4 showed higher discharge capacities compared to the cell with the PP separator for all C-rates tested. The good rate performance is an indication of not only higher ion conductivity in the hybrid membrane, but also lower interfacial resistance due to firm contacts between the hybrid membrane and electrode in the cell.

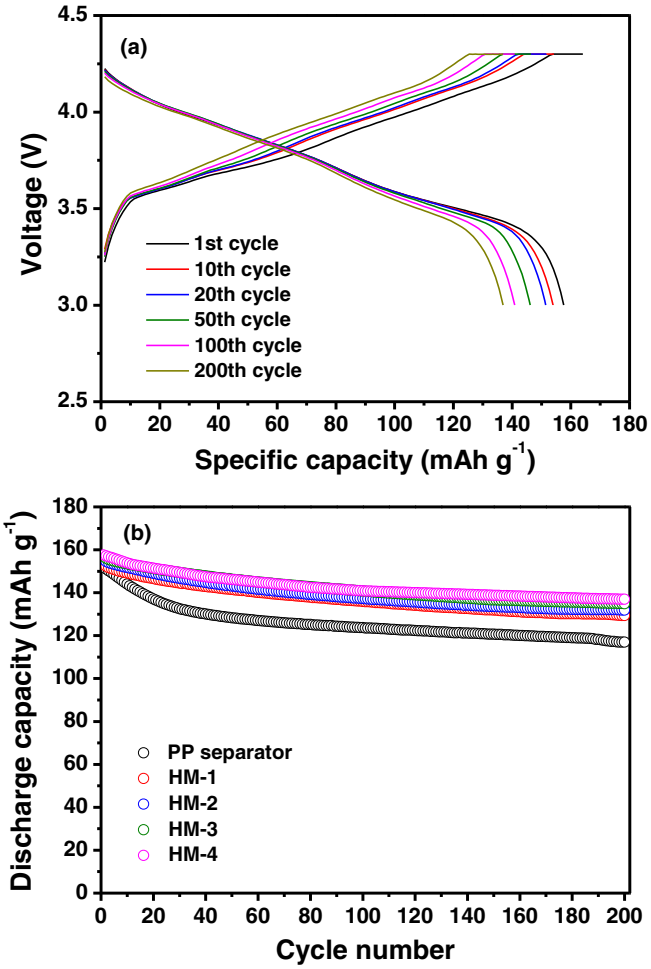

Figure 5. (a) Charge and discharge curves of the lithium-ion cell with hybrid membrane (HM-4) at 25°C (0.5 C CC and CV charge, 0.5 C CC discharge, cutoff voltage: 3.0–4.3 V), (b) discharge capacities of the lithium-ion cells assembled with PP separator and different hybrid membranes at 25°C.

A cycling test was also performed at 55°C to compare the cycling stability of the cells at high temperatures. Figure 7a shows the discharge capacities of the lithium-ion cells assembled with the PP separator and different hybrid membranes at 55°C. The cell with the PP separator suffered from large capacity fading, resulting in low capacity retention of 43.7% after 100 cycles. In contrast, the cells assembled with hybrid membranes exhibited better cycling stability. Among the cells with hybrid membranes, the cell assembled with HM-4 exhibited the best capacity retention. In order to examine the origin for differences in cycling performance at high temperature, the AC impedance spectra of the cells were obtained before and after repeated cycles at 55°C (Figures 7b and 7c). All of the spectra exhibited two overlapping semicircles, which could be assigned to the resistance of Li^+ ions through the solid electrolyte interphase film at the electrode surface and the charge transfer resistance at the electrode–electrolyte interface.[43,44] Before cycling (after two preconditioning cycles), the cells with hybrid membrane showed lower interfacial resistances to some extent due to the favorable interfacial contact. After 100 cycles, the electrolyte resistance corresponding to the high-frequency intercept at the real axis was higher in the cell with a PP separator. This result can be ascribed to lower ionic conductivity in the PP separator, loss of electrolyte solution due to leakage and deleterious reactions between the electrolyte and the electrodes during cycling. It was also found that the increase in interfacial resistances after cycling was much lower in the cells with hybrid membranes than the cell with a PP separator. This result implies that the cells with hybrid membranes

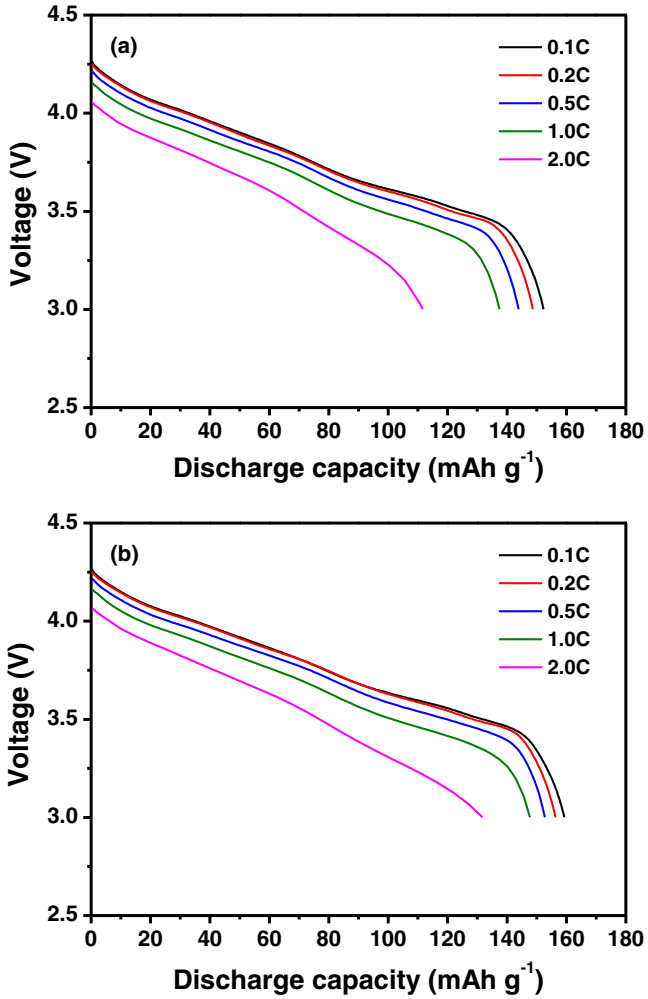

Figure 6. Discharge profiles of the lithium-ion cells assembled with (a) PP separator and (b) HM-4, as a function of the C rate at 25°C.

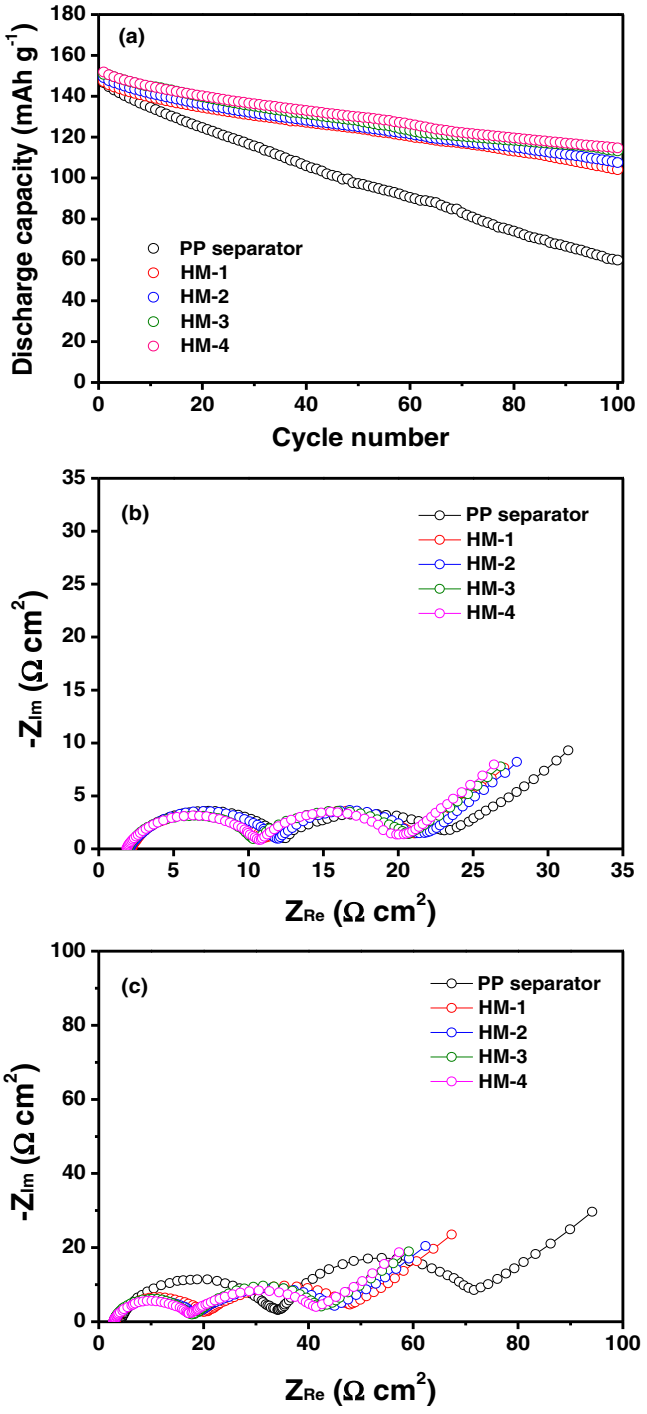

Figure 7. (a) Discharge capacities of the lithium-ion cells assembled with PP separator and different hybrid membranes at 55°C, as a function of the cycle number. AC impedance spectra of the lithium-ion cells with PP separator and different hybrid membranes, which were measured (b) before cycling (after preconditioning cycles) and (c) after 100 cycles at 55°C.

have more stable electrode–electrolyte interfaces, resulting in good capacity retention.

It is well known that high temperature cycling stability is closely related with the thermal stability of the electrolyte solution as well as the structural stability of cathode materials. To investigate the thermal stability of the $LiPF_6$-containing electrolyte employing PP separator and hybrid membrane at high temperature, we put a PP separator, hybrid membrane (HM-4) and LAGP powder in the electrolyte solution and kept them at 55°C for 1 week. As shown in Figure 8a, the electrolyte solution with the hybrid membrane or LAGP powder did not show any changes in color of the electrolyte solution after storage for 1 week at 55°C. In contrast, the electrolyte solution with a PP separator exhibited a pronounced color change to brown. It is well known that $LiPF_6$ salt can be thermally decomposed into gaseous PF_5 and LiF. The decomposed PF_5 is a very strong Lewis acid, which degrades the electrolyte solvents and thus changes its color to brown.[45,46] Hence, the above results indicate that the thermal stability of the electrolyte solution could be improved by using hybrid membranes containing LAGP instead of a PP separator. To investigate the reason for the improvement of the thermal stability of the electrolyte solution in the presence of a hybrid membrane, we measured the HF contents in the cells with the PP separator and hybrid membranes after storing the cells at 55°C for 1 week, and the results are shown in Figure 8b. It is evident that HF content was reduced in the cell with hybrid membranes. The PO_4^{3-} in the LAGP particle is a Lewis base that can complex with the reactive PF_5, which prevents PF_5 from being hydrolyzed to produce HF. Accordingly, the use of a hybrid membrane containing a high amount of LAPG particles inhibited the dissolution of transition metals from the active $LiNi_{0.5}Co_{0.2}Mn_{0.2}O_3$ material at elevated temperatures. As a result, the cells with hybrid membranes exhibited more stable cycling behavior, as the gradual capacity fading of layered $LiNi_xCo_yMn_{1-x-y}O_2$ materials at high temperatures arises from the dissolution of transition metals from the active cathode material by HF attack.[47,48]

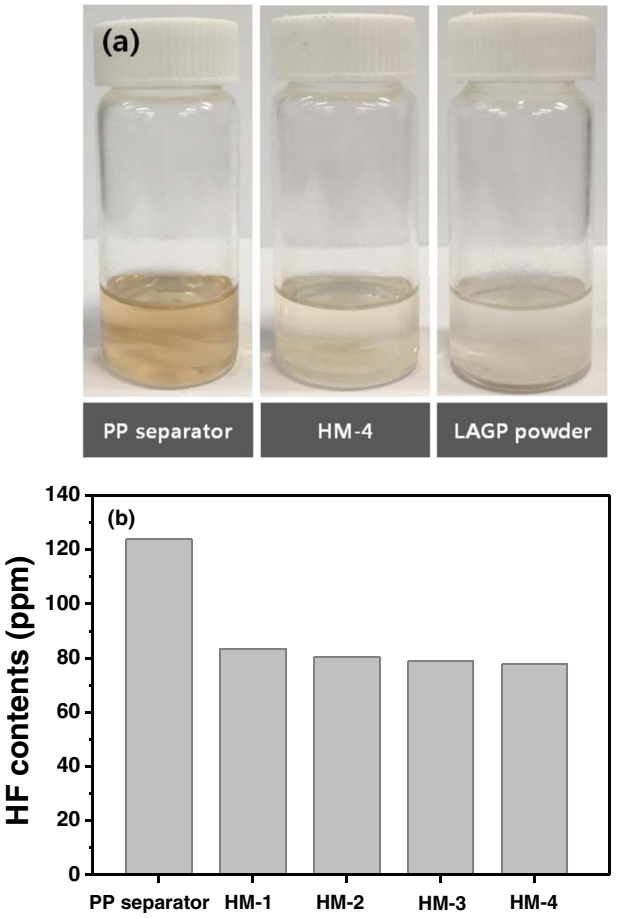

Figure 8. (a) Photographs of electrolyte solutions with PP separator, HM-4 and LAGP powder after storage at 150°C for 1 week and (b) HF contents in the cells with PP separator and different hybrid membranes after storing the cells at 55°C for 1 week.

Flammability of hybrid membrane and PP separator soaked with liquid electrolyte was compared. Figure 9 shows the photographic images of two samples obtained during flammability test. It confirmed that PP separator soaked with liquid electrolyte was flammable and its SET value was measured to be about 54 s g^{-1}. In contrast, only liquid electrolyte burned in the hybrid membrane soaked liquid electrolyte during flammability test, and the flame was extinguished after removing flame source. These results suggest that the use of hybrid membrane is very effective in reducing the flammability of the liquid electrolyte.

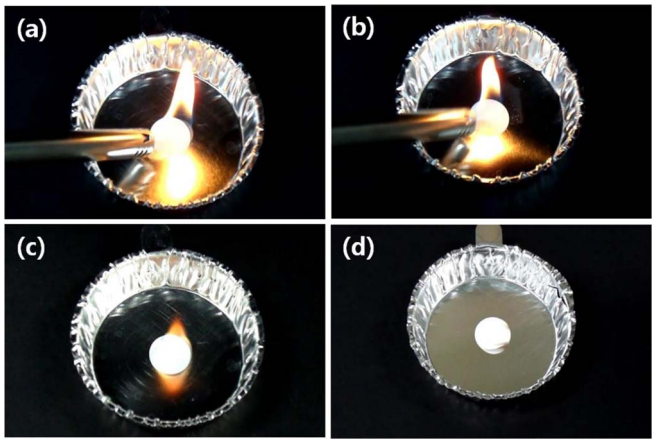

Figure 9. Photographic images of (a) PP separator and (b) hybrid membrane soaked with liquid electrolyte during ignition with flame source. (c) PP separator and (b) hybrid membrane after removing the flame source.

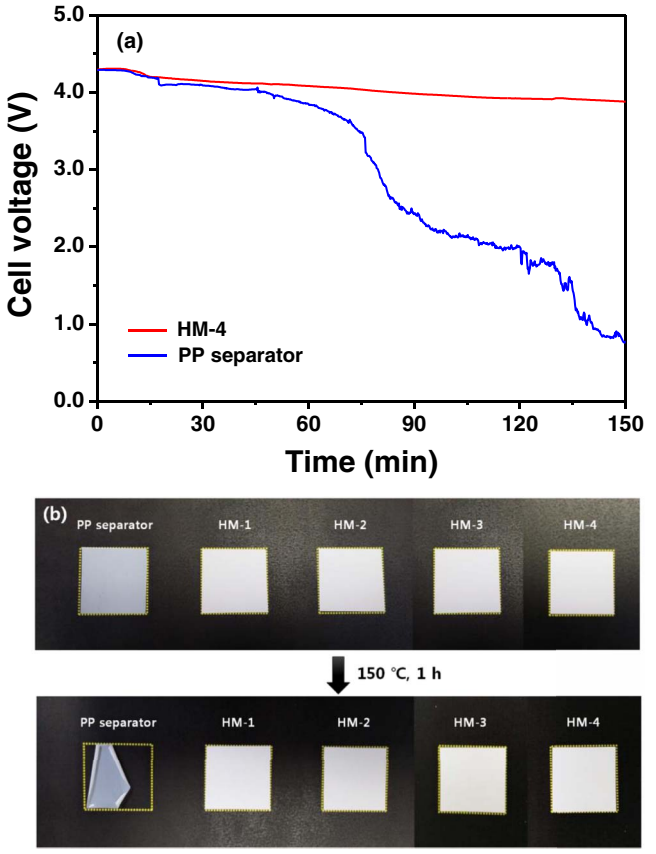

Figure 10. (a) Voltage profiles of the lithium-ion cells with PP separator and hybrid membrane (HM-4) during the hot oven test at 150°C for 150 min, and (b) photographs of the PP separator and different hybrid membranes before and after storage at 150°C for 1 h.

In order to compare the thermal safety of the cells with PP separator and hybrid membrane, the variations in cell voltages were monitored during heat exposure at 150°C. During this test, the cells assembled with PP separator and HM-4 were fully charged at room temperature, and their voltages were continuously monitored during storage in a hot oven at 150°C.[49,50] As a result, there were remarkable differences in voltage profiles between the cells assembled with PP separator and HM-4, as presented in Figure 10a. The voltage of the cell using PP separator gradually decreased with storage time. The voltage drop can be ascribed to internal short-circuits in the cell due to the thermal shrinkage of the PP separator at 150°C, as illustrated in Figure 10b. In contrast, the voltage of the cell with hybrid membrane maintained the initial voltage at first, and showed a slight drop without sudden voltage change during the test. This result is due to the fact that the presence of heat-resistant LAGP in the hybrid membranes could prevent dimensional changes at high temperatures (as shown in Figure 10b), which provided good protection against the short circuit of two electrodes in the cell at high temperatures. These results demonstrate that the enhanced thermal stability of hybrid membranes arising from the addition of LAGP powder allows fabrication of the lithium-ion cells with enhanced thermal safety.

Conclusions

Hybrid membranes composed of Li^+-conducting LAGP and P(VdF-co-HFP) were prepared in the form of a flexible thin film. By incorporating a large amount of LAGP in the hybrid membranes, ionic

conductivity and non-flammability could be improved. The lithium-ion cell employing the hybrid membrane composed of a graphite negative electrode and a $LiNi_{0.5}Co_{0.2}Mn_{0.3}O_2$ positive electrode delivered a high discharge capacity and exhibited good capacity retention at both ambient temperature and high temperature. The good cycling stability at high temperatures resulted from good interfacial contact of hybrid membranes with electrode and suppression of HF formation. The hybrid membrane integrated with the electrode also endowed the cell with high thermal resistance and thereby prevented an internal short circuit of the cell at high temperature.

Acknowledgments

The authors thank Samsung SDI for providing financial support.

References

1. M. Winter and R. J. Brodd, *Chem. Rev.*, **104**, 4245 (2004).
2. A. S. Arico, P. Bruce, B. Scrosati, J. -M. Tarascon, and W. V. Schalkwijk, *Nat. Mater.*, **4**, 366 (2005).
3. B. Dunn, H. Kamath, and J. -M. Tarascon, *Science*, **334**, 928 (2011).
4. V. Etacheri, R. Marom, R. Elazari, G. Salitra, and D. Aurbach, *Energy Environ. Sci.*, **4**, 3243 (2011).
5. B. Scrosati, J. Hassoun, and Y. K. Sun, *Energy Environ. Sci.*, **4**, 3287 (2011).
6. J. B. Goodenough and K. S. Park, *J. Am. Chem. Soc.*, **135**, 1167 (2013).
7. H. D. Yoo, E. Markevich, G. Salitra, D. Sharon, and D. Aurbach, *Materials Today*, **17**, 110 (2014).
8. D. Larcher and J. -M. Tarascon, *Nature Chem.*, **7**, 19 (2015).
9. S. Tobishima and J. Yamaki, *J. Power Sources*, **81–82**, 882 (1999).
10. G. Venugopal, J. Moore, J. Howard, and S. Pendalwar, *J. Power Sources*, **77**, 34 (1999).
11. I. Uchida, H. Ishikawa, M. Mohamedi, and M. Umeda, *J. Power Sources*, **119–121**, 821 (2003).
12. M. S. Wu, P. C. J. Chiang, J. C. Lin, and Y. S. Jan, *Electrochim. Acta*, **49**, 1803 (2004).
13. J. Saunier, F. Alloin, J. Y. Sanchez, and G. Caillon, *J. Power Sources*, **119–121**, 454 (2003).
14. P. Knauth, *Solid State Ionics*, **180**, 911 (2009).
15. J. W. Fergus, *J. Power Sources*, **195**, 4554 (2010).
16. E. Quartarone and P. Mustarelli, *Chem. Soc. Rev.*, **40**, 2525 (2011).
17. M. Nagao, H. Kitaura, A. Hayashi, and M. Tatsumisago, *J. Electrochem. Soc.*, **160**, A819 (2013).
18. L. Damen, J. Hassoun, M. Mastragostino, and B. Scrosati, *J. Power Sources*, **195**, 6902 (2010).
19. T. Inada, K. Takada, A. Kajiyama, M. Kouguchi, H. Sasaki, S. Kondo, M. Watanabe, M. Murayama, and R. Kanno, *Solid State Ionics*, **158**, 275 (2003).
20. K. M. Nairn, A. S. Best, P. J. Newman, D. R. MacFarlane, and M. Forsyth, *Solid State Ionics*, **121**, 115 (1999).
21. C. Wang, X. W. Zhang, and A. J. Appleby, *J. Electrochem. Soc.*, **152**, A205 (2005).
22. Y. Inda, T. Katoh, and M. Baba, *J. Power Sources*, **174**, 741 (2007).
23. Y. C. Jung, S. M. Lee, J. H. Choi, S. S. Jang, and D. W. Kim, *J. Electrochem. Soc.*, **162**, A704 (2015).
24. N. M. Asl, J. Keith, C. Lim, L. Zhu, and Y. Kim, *Electrochim. Acta*, **79**, 8 (2012).
25. Y. C. Jung, S. K. Kim, M. S. Kim, J. H. Lee, M. S. Han, D. H. Kim, W. C. Shin, M. Ue, and D. W. Kim, *J. Power Sources*, **293**, 675 (2015).
26. I. Pinnau and W. J. Koros, *J. Applied Polymer Science*, **43**, 1491 (1991).
27. X. Huang, *J. Power Sources*, **196**, 8125 (2011).
28. A. Manuel Stephan and D. Teeters, *Electrochim. Acta*, **48**, 2143 (2003).
29. R. Miao, B. Liu, Z. Zhu, Y. Liu, J. Li, X. Wang, and Q. Li, *J. Power Sources*, **184**, 420 (2008).
30. K. Takada, *Acta Materialia*, **61**, 759 (2013).
31. H. S. Jadhav, M. S. Cho, R. S. Kalubarme, J. S. Lee, K. N. Jung, K. H. Shin, and C. J. Park, *J. Power Sources*, **241**, 502 (2013).
32. C. G. Wu, M. I. Lu, and H. J. Chuang, *Polymer*, **46**, 5929 (2005).
33. T. Ma, Z. Cui, Y. Wu, S. Qin, H. Wang, F. Yan, N. Han, and J. Li, *J. Membr. Sci.*, **444**, 213 (2013).
34. J. R. Kim, S. W. Choi, S. M. Jo, W. S. Lee, and B. C. Kim, *J. Electrochem. Soc.*, **152**, A295 (2005).
35. S. M. Park, Y. S. Lee, and D. W. Kim, *J. Electrochem. Soc.*, **162**, A3071 (2015).
36. K. Xu, M. S. Ding, S. Zhang, J. L. Allen, and T. R. Jow, *J. Electrochem. Soc.*, **149**, A622 (2002).
37. Y. S. Yun, J. H. Kim, S. Y. Lee, E. G. Shim, and D. W. Kim, *J. Power Sources*, **196**, 6750 (2011).
38. Y. K. Sun, K. J. Hong, J. Prakash, and K. Amine, *Electrochem. Commun.*, **4**, 344 (2002).
39. T.-H. Cho, M. Tanaka, H. Onishi, Y. Kondo, T. Nakamura, H. Yamazaki, S. Tanase, and T. Sakai, *J. Power Sources*, **181**, 155 (2008).
40. B. V. R. Chowdari, G. V. Subba Rao, and G. Y. H. Lee, *Solid State Ionics*, **136–137**, 1067 (2000).
41. J. Fu, *Solid State Ionics*, **104**, 191 (1997).
42. W. Z. Ma, J. Zhang, S. J. Chen, and X. L. Wang, *Appl. Surf. Sci.*, **254**, 5635 (2008).
43. Y. Bai, X. Wang, X. Zhang, H. Shu, X. Yang, B. Hu, Q. Wei, H. Wu, and Y. Song, *Electrochim. Acta*, **109**, 355 (2013).
44. T. Liu, A. Garsuch, F. Chesneau, and B. L. Lucht, *J. Power Sources*, **269**, 920 (2014).
45. S. E. Sloop, J. B. Kerr, and K. Kinoshita, *J. Power Sources*, **119–121**, 330 (2003).
46. C. L. Campion, W. T. Li, and B. L. Lucht, *J. Electrochem. Soc.*, **152**, A2327 (2005).
47. G. G. Amatucci, J. M. Tarascon, and L. C. Klein, *Solid State Ionics*, **83**, 167 (1996).
48. S. U. Woo, B. C. Park, C. S. Yoon, S. T. Myung, J. Prakash, and Y. K. Sun, *J. Electrochem. Soc.*, **154**, A649 (2007).
49. J. Song, M. H. Ryou, B. Son, J. N. Lee, D. J. Lee, Y. M. Lee, J. W. Choi, and J. K. Park, *Electrochim. Acta*, **85**, 524 (2012).
50. T. H. Cho, M. Tanaka, H. Onishi, Y. Kondo, T. Nakamura, H. Yamazaki, S. Tanase, and T. Sakai, *J. Power Sources*, **181**, 155 (2008).